

**High performance of catalysts supported by directly grown PTFE-free micro-porous CNT layer in a proton exchange membrane fuel cell†**He-Yun Du,<sup>a</sup> Chen-Hao Wang,<sup>\*b</sup> Hsin-Cheng Hsu,<sup>c</sup> Sun-Tang Chang,<sup>c</sup> Shi-Chern Yen,<sup>a</sup> Li-Chyong Chen,<sup>c</sup> Balasubramanian Viswanathan<sup>d</sup> and Kuei-Hsien Chen<sup>\*ce</sup>

Received 25th September 2010, Accepted 10th November 2010

DOI: 10.1039/c0jm03215h

A proton exchange membrane fuel cell (PEMFC) uses a solid polymer electrolyte, *viz.* Nafion®, sandwiched between the two electrodes. Nafion® not only plays the role as an electronic insulator and gas barrier but also allows rapid proton transport and supports high current densities. In order to maintain the high proton conductivity of Nafion®, humidified H<sub>2</sub> and O<sub>2</sub> are passed through the two electrodes. However, water gets easily condensed in the electrodes. This process, called water-flooding, degrades the performance of PEMFC. Hence, a hydrophobic agent, *viz.* polytetrafluoroethylene (PTFE), is normally incorporated into the electrodes to prevent this phenomenon. Since it is electrically insulating, the incorporation of PTFE increases the internal resistance of the fuel cell. In this study, we successfully demonstrate a PEMFC with catalyst layer comprising of low loading of platinum nanoparticles (0.05 mg cm<sup>-2</sup>) supported by a directly grown micro-porous carbon nanotube (CNT) layer without incorporation of PTFE, (Pt/MPL-CNT). This cell performs well without exhibiting water-flooding. A commercial electrode, the catalyst layer of which was supported by a conventional micro-porous layer of carbon black mixed with 30 w.t.% PTFE, was used as a reference (Pt/PTFE-MPL-CB). In the single cell tests, PEMFCs with 0.05 mg cm<sup>-2</sup> Pt/MPL-CNT and 0.25 mg cm<sup>-2</sup> Pt/PTFE-MPL-CB were used at the cathodes. These cells yielded maximum power densities of 902 mW cm<sup>-2</sup> and 824 mW cm<sup>-2</sup>, respectively, at 70 °C when operated with H<sub>2</sub>/O<sub>2</sub>. Notably, the Pt-loading of Pt/MPL-CNT cell is one-fifth of that of Pt/PTFE-MPL-CB, but the former still outperforms the latter. It is shown that the directly grown micro-porous CNT layer has low electronic resistance and is intrinsically hydrophobic, which are the properties responsible for the high performance obtained here.

**Introduction**

The proton exchange membrane fuel cell (PEMFC) consists of a sandwiched structure, wherein a Nafion® membrane is sandwiched between two catalyst layers. A fuel cell is considered to be a viable future power source because of its low operating temperature, high power density and environmentally friendly

technology.<sup>1,2</sup> The power-generating unit is a catalyst layer, which comprises of porous carbon black (such as Vulcan XC-72) and supporting platinum catalysts, and converts chemical energy to electrical energy.<sup>3,4</sup> To maintain high proton conductivity of the Nafion® membrane, which depends on a high level of hydration, humidified gas (H<sub>2</sub> and O<sub>2</sub>) must be fed into the PEMFC; however, the electrodes may undergo water-flooding, which slows down the redox reaction.<sup>5</sup> Efforts to improve resistance to water-flooding have focused on (1) impregnating the pores of the gas diffusion layer (GDL) with hydrophobic agents (such as polytetrafluoroethylene, PTFE) and (2) addition of a micro-porous layer (MPL) of carbon black mixed with hydrophobic agents between the catalyst layer and the GDL.<sup>6</sup> Various treatments to optimize in-plane electrical resistivity, hydrophobicity, gas permeability and pore size distribution have revealed that incorporation of an MPL can reduce water-flooding and increase the catalytic utilization.<sup>7-9</sup> However, previous attempts have focused on incorporation of an electrically insulating hydrophobic agent, *viz.* PTFE, into the MPL, to isolate the carbon black and block pores, detrimentally affecting electron transfer and gas/liquid transfer in the electrode.

<sup>a</sup>Department of Chemical Engineering, National Taiwan University, 106 Taipei, Taiwan<sup>b</sup>Department of Materials Science and Engineering, National Taiwan University of Science and Technology, 106 Taipei, Taiwan. E-mail: chwang@mail.ntust.edu.tw; Fax: +886-2-27376544; Tel: +886-2-27303715<sup>c</sup>Center for Condensed Matter Sciences, National Taiwan University, 106 Taipei, Taiwan<sup>d</sup>National Center for Catalysis Research, Indian Institute of Technology Madras, Chennai, 600 036, India<sup>e</sup>Institute of Atomic and Molecular Sciences, Academia Sinica, Taipei, 106, Taiwan. E-mail: chenkh@pub.iams.sinica.edu.tw; Fax: +886-2-23620200; Tel: +886-2-23668232

† Electronic supplementary information (ESI) available. See DOI: 10.1039/c0jm03215h

Some studies have demonstrated the use of various carbon blacks in the MPL to improve the electrical performance and wetting behavior of PEMFCs.<sup>10–12</sup> Kannan *et al.* used CNTs rather than carbon black in the MPL, improving the fuel cell performance.<sup>13</sup> The CNT-based components exhibit excellent GDL surface morphology and uniform distribution of platinum catalyst over the CNTs support. Wu *et al.* added CNTs to the MPL and demonstrated reduction in the water-crossover flux, that in-turn allowed the direct methanol fuel cell to be operated at a higher methanol concentration, improving the fuel cell performance.<sup>14</sup> However, in all the above studies, PTFE was incorporated into the MPLs, which reduced its electrical conductivity. Additionally, the conventional MPL was sandwiched between the catalyst layer and the GDL. In such a structure, when electrons are transferred from the catalyst *via* the MPL to the GDL, they lose energy at each interface.

In this study, a micro-porous CNT layer was directly grown on a carbon cloth (MPL-CNT), and Pt catalysts were subsequently deposited on the MPL-CNT (Pt/MPL-CNT), as shown in detail in Scheme 1. The MPL-CNT has excellent electron conductivity and is intrinsically hydrophobic. It is, thus, superior to the conventional MPL. The MPL-CNT not only supports Pt catalysts and distributes gas/liquid access path but also provides a direct pathway for electron transfer, such that the deposited Pt catalysts are almost guaranteed to be in electrical contact with the external circuit.

## Experimental

### Fabrication of Pt/MPL-CNT electrode

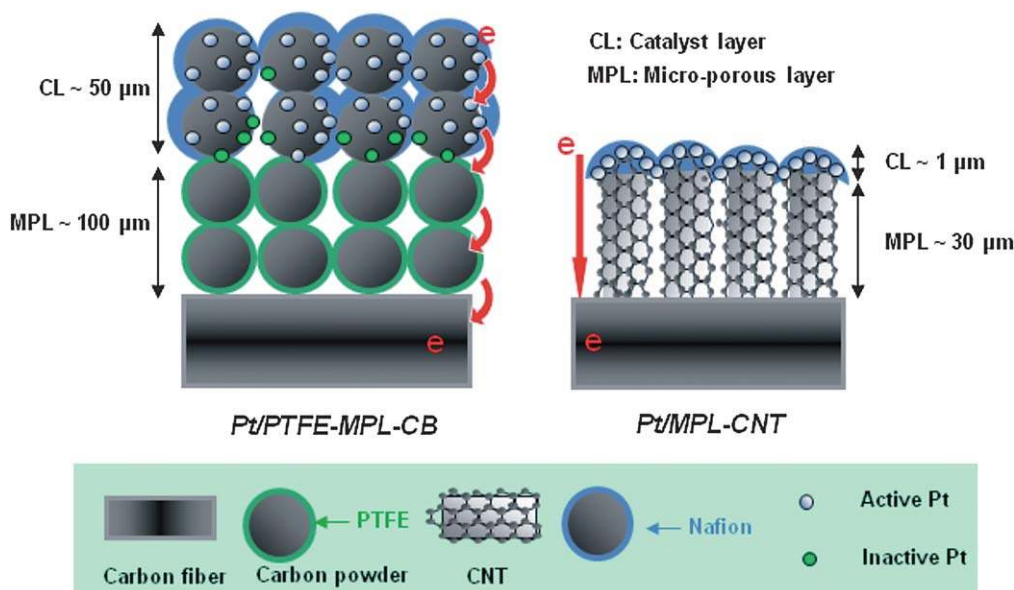
The micro-porous CNT layer was directly grown on a carbon cloth by cobalt-assisted catalytic growth using the microwave plasma-enhanced chemical vapor deposition method. The sol-gel solution of cobalt(III) nitrate in isopropanol was spread uniformly on the carbon cloth using a spin coater, and was then dried by natural convection. Before CNT growth, the carbon

cloth was treated with hydrogen plasma at a microwave power of 1 kW and a chamber pressure of 28 Torr for 10 min, not only to clean the sample surface but also to transform the cobalt catalyst layer into nanoparticles. CNTs were synthesized in mixed precursors ( $\text{CH}_4/\text{H}_2/\text{N}_2$ : 20/80/80), at a microwave power of 2 kW, a chamber pressure of 40 Torr, and a substrate temperature of 900 °C for 10 min.

For preparation of Pt catalysts supported on the MPL-CNT, physical vapor deposition (PVD) was used to sputter platinum onto the template to form Pt/MPL-CNT. For comparison, the catalysts were also sputtered on a carbon cloth without a micro-porous CNT layer, to form Pt/CC. The platinum target was placed in the radio-frequency planar magnetron sputtering gun in a PVD system. The deposition was carried out in an argon atmosphere at a working pressure of  $5 \times 10^{-2}$  Torr to yield a highly uniform coating of nanoscale Pt catalysts on MPL-CNT. High-resolution scanning electron microscopy (HRSEM, JEOL-6700F) was used to elucidate the micro-structural surface morphologies of MPL-CNT and Pt/MPL-CNT. Backscattering electron images were obtained using an r-filter accessory. Transmission electron microscopy (TEM, JEOL-2100) was employed to capture images of CNTs and the Pt catalysts. The wetting ability of the MPL-CNT was evaluated by measuring the contact angle of water (Face CA-D, Kyowa Interface Science). The surface area and porosity were measured using a specific area and pore size distribution instrument (Tristar, Micrometry). The magnitude of metal loading (weight per unit area) was determined by using inductively coupled plasma-optical emission spectroscopy (ICP-OES, Perkin-Elmer ICP-OES Optima 3000).

### Fuel cell performance test

The membrane-electrode-assemblies (MEAs) were tested on a 2.25 cm<sup>2</sup> single cell. As a reference, 0.25 mg cm<sup>-2</sup> Pt/C were loaded on the conventional MPL using carbon black that had been mixed with 30 wt.% PTFE (Pt/PTFE-MPL-CB) in MEAs.



**Scheme 1** Schematic diagram of the Pt/PTFE-MPL-CB and the Pt/MPL-CNT.

For all MEAs, commercial gas diffusion electrodes ( $0.25 \text{ mg cm}^{-2}$  Pt/C, E-TEK) were used as anodes. Each MEA was prepared by hot-pressing the electrodes on each side of Nafion® 212 ( $\text{H}^+$ , DuPont) membrane—at  $135 \text{ }^\circ\text{C}$  and  $130 \text{ kg cm}^{-2}$  for 2 min.

In the polarization test, high-purity hydrogen and oxygen at flow rates of 200 standard cubic centimetres per minute (SCCM) and 400 SCCM, respectively, were fed to the anode and the cathode. Both gases were passed through a humidifier (operated at  $70 \text{ }^\circ\text{C}$ ), before they entered the MEA. A single cell was tested in a PEMFC test station (Asia Pacific Fuel Cell Technologies Ltd.) and the back pressure gauges of both electrodes read 1 atm. The polarization curves were plotted as cell voltage against steady state current. The AC impedance of MEAs was analyzed using a Solartron electrochemical test system (SI 1280Z).

## Results and discussion

Fig. 1a and 1b present HRSEM images of the original carbon cloth and as-grown MPL-CNT, respectively. It can be readily

seen that many CNTs were directly grown on the carbon cloth, forming a continuous CNT layer. Fig. 1c reveals that the CNT layer completely covers the carbon fibers of the carbon cloth and fills the vacancies between the carbon fibers, indicating that the CNT layer consists of numerous microscopic pores that make it accessible to gas and liquid. As-grown CNT, the TEM image of which is presented in Fig. 1d, has a multiwall, bamboo-like structure, which has been observed previously.<sup>15,16</sup> The HRTEM image in Fig. 1e demonstrates that Pt nanoparticles are uniformly deposited on the CNT surface, with an average diameter of around 5 nm.

Since the PEMFC requires water to maintain its proton conductivity, hydrogen and oxygen (or air) are normally fed at 100% relative humidity to the MEA. However, water readily condenses and fills the pores in the catalyst layer, thereby causing water flooding. The MPL reported here, however, consists of proper pore structure and hydrophobicity that enables improved gas transport and removal of water from the catalyst layer. The hydrophobicity of MPL was determined by measuring the water contact angle. Fig. 2 shows that the contact angles on

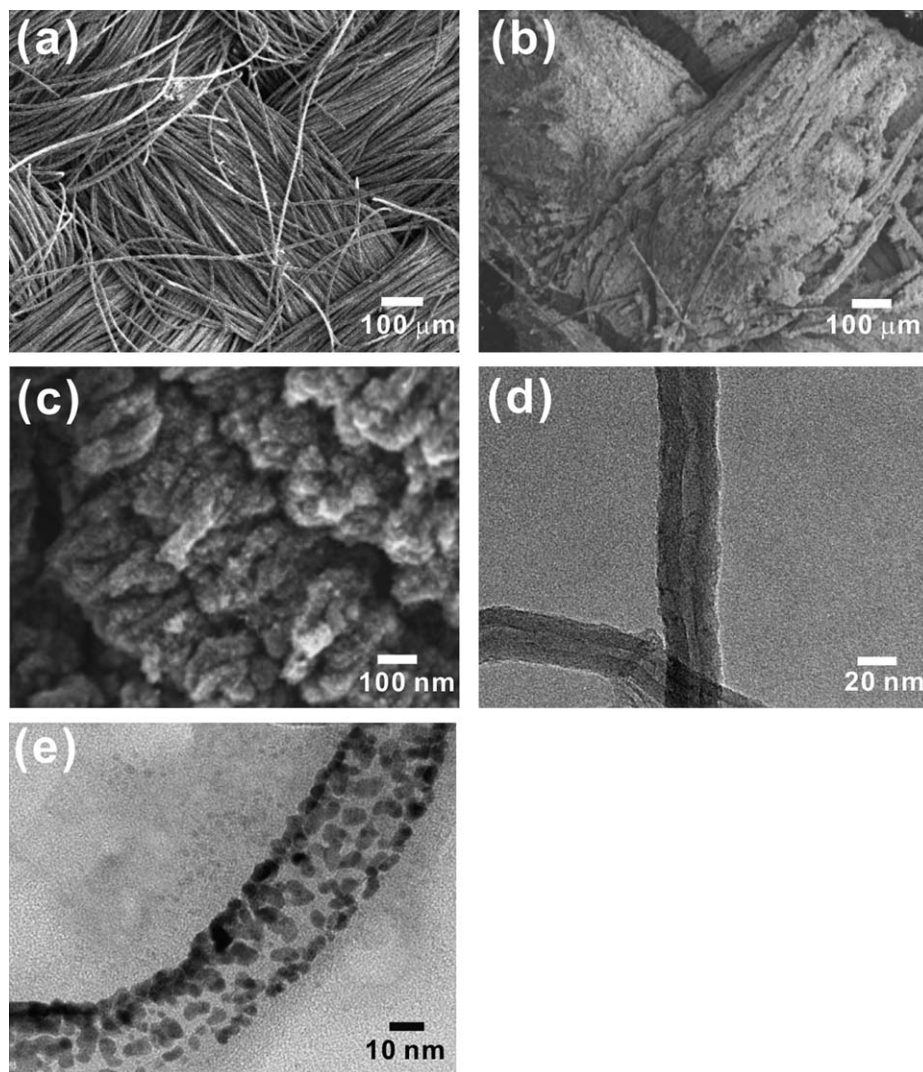


**Fig. 1** Electron microscope images showing (a) the original carbon cloth; (b) the CNTs directly-grown on carbon cloth (MPL-CNT); (c) the magnified image of the MPL-CNT; (d) TEM image of as-grown CNT structure, and (e) Pt nanoparticles deposited on the CNT.

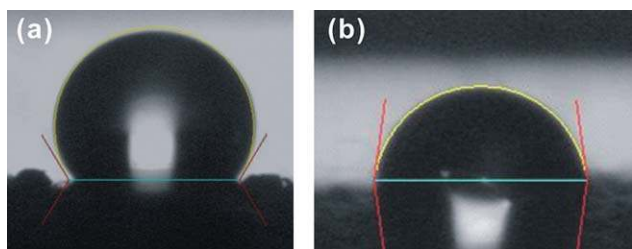


**Fig. 2** Wetting angle images of (a) the MPL-CNT (b) the original carbon cloth.

the MPL-CNT and original carbon cloth are  $120.81^\circ$  and  $82.47^\circ$ , respectively, indicating that the MPL-CNT has a strong intrinsic hydrophobic property, which prevents flooding of the gas/liquid flow channels with water.

Capillary-driven liquid flow through diffusion media may dominate fuel cell operation, especially in an oversaturated system. According to the Young–Laplace equation, the radius of a pore is related to the capillary pressure and wetting ability of a pore by,

$$P_c = \frac{2\gamma\cos\theta}{r} \quad (\text{Eq. 1})$$

where  $\gamma$  is the surface energy of water;  $\theta$  represents the contact angle between water and surface of the pore;  $P_c$  is the capillary pressure, and  $r$  is the radius of the pores. In hydrophobic GDL, the capillary pressure is negative; therefore, the liquid pressure exceeds the gas-phase pressure. Pasaogullari *et al.* suggested that capillary transport is the dominant transport process by which water is removed from flooded GDLs.<sup>17</sup> Moreover, the liquid pressure increases with the proportion of the void spaces that are occupied by liquid water; therefore, a liquid pressure gradient is established from regions of greater liquid saturation to those of lower liquid saturation. This pressure gradient drives liquid water flow. A higher contact angle is associated with higher capillary pressure, and therefore a higher water removal rate. The MPL-CNT system establishes a pressure gradient that enables removal of water from the catalyst layer. BET measurements demonstrate that the MPL-CNT has a total surface area of  $122.9 \text{ m}^2 \text{ g}^{-1}$ , including a micro-pore surface area of  $28.13 \text{ m}^2 \text{ g}^{-1}$ . This large surface area favors subsequent catalyst loading. Tian *et al.* manipulated the relation of PTFE and carbon powder by the microwave-assisted method, indicating the decrease of BET surface area with the incorporation of PTFE.<sup>18</sup> A PTFE-free MPL-CNT, with high BET surface area not only possesses a suitable porosity for providing effective liquid transport pathways but also supports catalysts more effectively.

Fig. 3a and 3b present cross-sectional HESEM backscattering electron images (BEI) of Pt/MPL-CNT and Pt/PTFE-MPL-CB MEAs, respectively. The intensity of backscattered electrons is particularly sensitive to atomic number, the larger the atomic number, the brighter it appears in the BEI, thus enhancing the atomic contrast. Since Pt has much greater atomic number than C, the bright regions in the BEI are mostly attributed to Pt. Due to the large atomic number difference between Pt and C, the contrast between catalyst layer and micro-porous layer can be differentiated clearly in the BEI. The catalyst layer in Pt/MPL-CNT is very thin—only 2 to 5  $\mu\text{m}$  thick—and is deposited on the

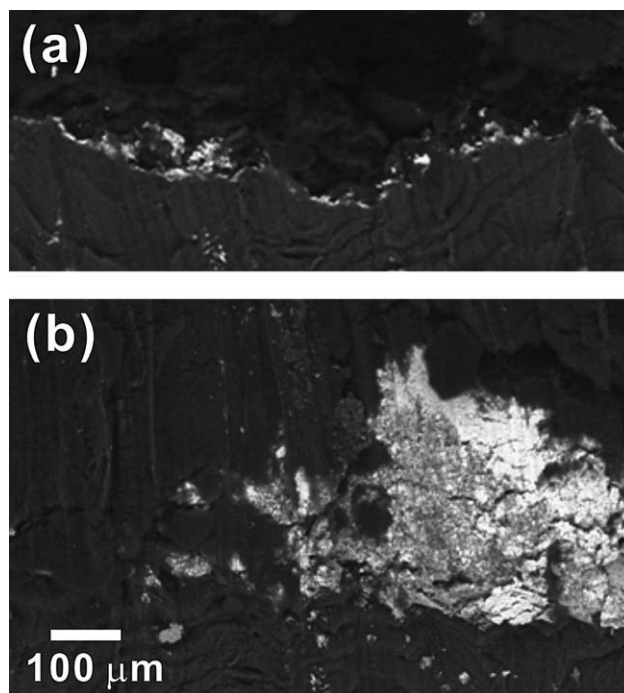


**Fig. 3** Cross-sectional MEAs viewed by HRSEM backscattering electron images showing (a)  $0.05 \text{ mg cm}^{-2}$  Pt/MPL-CNT and (b)  $0.25 \text{ mg cm}^{-2}$  Pt/PTFE-MPL-CB. The bright regions represent the catalyst layers.

MPL-CNT. It also forms a continuous interface with the MPL-CNT, which promotes not only the catalyst distribution but also the catalytic utilization. On the other hand, the catalyst layer in the Pt/PTFE-MPL-CB system is 50  $\mu\text{m}$  thick, and forms a discontinuous interface, resulting in the inefficient catalytic utilization. Additionally, it leads to serious agglomeration of Pt catalysts, which reduces the catalytic utilization.

Fig. 4 presents the polarization curves for MEAs with Pt/MPL-CNT, Pt/PTFE-MPL-CB and Pt/CC. The highest power densities achieved with these MEAs are 902, 824 and 412  $\text{mW cm}^{-2}$ , respectively. Water-flooding is known to occur in the cathode, but the PTFE-free Pt/MPL-CNT MEA exhibited no obvious water-flooding in the fuel cell test. Since the oxygen reduction reaction is slower than the hydrogen oxidation reaction, the cathode requires a higher Pt loading to maintain a high reaction rate. In this study, Pt/MPL-CNT had only one fifth of the Pt loading of Pt/PTFE-MPL-CB but outperformed them in terms of power generation. Besides, the electrochemical surface areas of Pt/MPL-CNT MEA and Pt/PTFE-MPL-CB MEA demonstrate  $141.5 \text{ cm}^2$  and  $125.9 \text{ cm}^2$ , respectively, indicating that the former has more efficient catalytic utilization than the latter. (See the experimental setup and Fig. S3 in the ESI†). The internal resistance of MEA is one of the important factors that significantly affects fuel cell performance. The slope of the polarization curve between 0.7 and 0.4 V is related to ohmic loss, which is primarily determined by the internal resistance that is comprised of electronic, ionic and contact resistances. The absolute slope of the curve for Pt/MPL-CNT is much lower than those for Pt/PTFE-MPL-CB as well as Pt/CC, indicating that the former has lower internal resistance. To determine the magnitude of internal resistance, AC impedance of the MEAs consisting of Pt/MPL-CNT and Pt/PTFE-MPL-CB were measured at 20 000 Hz, which

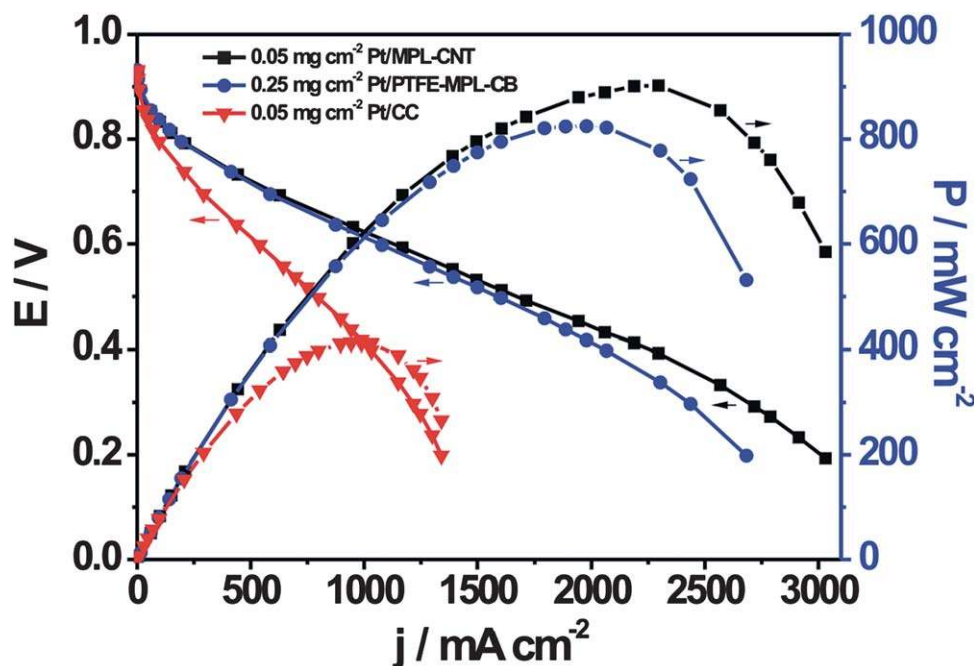


Fig. 4 Polarization curves of the MEAs using  $0.05 \text{ mg cm}^{-2}$  Pt/MPL-CNT,  $0.25 \text{ mg cm}^{-2}$  Pt/PTFE-MPL-CB and  $0.05 \text{ mg cm}^{-2}$  Pt/CC as cathodes.

yielded the values of  $0.26 \Omega \text{ cm}^2$  and  $0.79 \Omega \text{ cm}^2$ , respectively. Clearly, the MEA with Pt/MPL-CNT has a lower resistance, presumably owing to the higher conductivity of CNT without additional PTFE incorporation, a contiguous catalyst layer, and its low electron-transfer barrier between interfaces.

Clearly, the MEA based on Pt/MPL-CNT outperforms those using either Pt/PTFE-MPL-CB or Pt/CC, for the following reasons. First, nanoscopic Pt nanoparticles are uniformly dispersed on the CNT surface, providing a large surface area for the chemical reactions to occur. Second, the MPL-CNT, in which CNTs are directly grown on a carbon cloth, provides a direct electron-transfer pathway, reducing energy-losses between interfaces. Third, the MEA with Pt/MPL-CNT has a much thinner catalyst layer than a conventional electrode, providing shorter pathways for mass-transfer as well as electron-transfer. Fourth, Pt/MPL-CNT possesses a contiguous catalyst layer, which is favorable to the catalytic utilization. Fifth, owing to the intrinsic hydrophobic property and porosity of MPL-CNT, the MEA based on Pt/MPL-CNT not only supports the catalyst but also acts as a water-managing agent without the incorporation of PTFE.

## Conclusions

A high-performance composite electrode structure, Pt/MPL-CNT, with low Pt catalyst loading was successfully developed in this study. This Pt/MPL-CNT structure consists of a thin catalyst layer, which is intrinsically hydrophobic, and has high electrical conductivity, a low electron-transfer barrier and a contiguous interface layer, resulting in excellent performance.

## Acknowledgements

The authors would like to thank the Ministry of Education, Academia Sinica, and the National Science Council of Taiwan

for financially supporting this research. Technical support from NanoCore, the Core facilities for nanoscience and nanotechnology at Academia Sinica in Taiwan, is acknowledged.

## References

- 1 S. J. C. Cleghorn, X. Ren, T. E. Springer, M. S. Wilson, C. Zawodzinski, T. A. Zawodzinski and S. Gottesfeld, *Int. J. Hydrogen Energy*, 1997, **22**, 1137–1144.
- 2 V. Mehta and J. S. Cooper, *J. Power Sources*, 2003, **114**, 32–53.
- 3 X. Wang, H. Zhang, J. Zhang, H. Xu, X. Zhu, J. Chen and B. Yi, *J. Power Sources*, 2006, **162**, 474–479.
- 4 X. L. Wang, H. M. Zhang, J. L. Zhang, H. F. Xu, Z. Q. Tian, J. Chen, H. X. Zhong, Y. M. Liang and B. L. Yi, *Electrochim. Acta*, 2006, **51**, 4909–4915.
- 5 T. A. Zawodzinski, J. Davey, J. Valerio and S. Gottesfeld, *Electrochim. Acta*, 1995, **40**, 297–302.
- 6 S. Park, J.-W. Lee and B. N. Popov, *J. Power Sources*, 2006, **163**, 357–363.
- 7 J. H. Nam, K.-J. Lee, G.-S. Hwang, C.-J. Kim and M. Kaviany, *Int. J. Heat Mass Transfer*, 2009, **52**, 2779–2791.
- 8 J. T. Gostick, M. A. Ioannidis, M. W. Fowler and M. D. Pritzker, *Electrochim. Commun.*, 2009, **11**, 576–579.
- 9 S. Park, J.-W. Lee and B. N. Popov, *J. Power Sources*, 2008, **177**, 457–463.
- 10 T. F. Hung, J. Huang, H. J. Chuang, S. H. Bai, Y. J. Lai and Y. W. Chen-Yang, *J. Power Sources*, 2008, **184**, 165–171.
- 11 J. Chen, H. Xu, H. Zhang and B. Yi, *J. Power Sources*, 2008, **182**, 531–539.
- 12 C.-H. Liu, T.-H. Ko and Y.-K. Liao, *J. Power Sources*, 2008, **178**, 80–85.
- 13 A. M. Kannan, V. P. Veedu, L. Munukutla and M. N. Ghasemi-Nejhad, *Electrochim. Solid-State Lett.*, 2007, **10**, 47–50.
- 14 Q. X. Wu, T. S. Zhao, R. Chen and W. W. Yang, *J. Power Sources*, 2009, **191**, 304–311.
- 15 C. H. Wang, H. Y. Du, Y. T. Tsai, C. P. Chen, C. J. Huang, L. C. Chen, K. H. Chen and H. C. Shih, *J. Power Sources*, 2007, **171**, 55–62.
- 16 C.-H. Wang, H.-C. Shih, Y.-T. Tsai, H.-Y. Du, L.-C. Chen and K.-H. Chen, *Electrochim. Acta*, 2006, **52**, 1612–1617.
- 17 U. Pasaogullari and C. Y. Wang, *J. Electrochem. Soc.*, 2004, **151**, A399–A406.
- 18 Z. Q. Tian, X. L. Wang, H. M. Zhang, B. L. Yi and S. P. Jiang, *Electrochim. Commun.*, 2006, **8**, 1158–1162.